

RESEARCH ARTICLE

10.1002/2014JC010382

Key Points:

- An approach to derive ITF proxy from satellite SSH and OBP data is shown
- Makassar data are used to find the optimal locations in the theoretical formula
- For the first time, a longest ITF transport proxy since 1992 is derived

Correspondence to:

R. D. Susanto
dwi@atmos.umd.edu

Citation:

Susanto, R. D., and Y. T. Song (2015), Indonesian throughflow proxy from satellite altimeters and gravimeters, *J. Geophys. Res. Oceans*, 120, doi:10.1002/2014JC010382.

Received 12 AUG 2014

Accepted 10 MAR 2015

Accepted article online 25 MAR 2015

Indonesian throughflow proxy from satellite altimeters and gravimeters

R. Dwi Susanto^{1,2} and Y. Tony Song³

¹Department of Atmospheric and Oceanic Science, University of Maryland, College Park, Maryland, USA, ²Center for Oceanography and Marine Technology, Surya University, Tangerang, Indonesia, ³Jet Propulsion Laboratory, California Institute of Technology, Pasadena, California, USA

Abstract The Indonesian throughflow (ITF) from the Pacific to the Indian Ocean plays an important role in global ocean circulation and climate. Yet, continuous ITF measurement is difficult and expensive. The longest time series of in situ measurements of the ITF to date were taken in the Makassar Strait, the main pathway of the ITF. Here we have demonstrated a plausible approach to derive the ITF transport proxy using satellite altimetry sea surface height (SSH), gravimetry ocean bottom pressure (OBP) data, in situ measurements from the Makassar Strait from 1996 to 1998 and 2004 to 2011, and a theoretical formulation. We first identified the optimal locations of the correlation between the observed ITF transport through the Makassar Strait and the pressure gradients, represented by the SSH and OBP differences between the Pacific and Indian Oceans at a $1^\circ \times 1^\circ$ horizontal resolution. The optimal locations were found centered at 162°E and 11°N in the Pacific Ocean and 80°E and 0° in the Indian Ocean, then were used in the theoretical formulation to estimate the throughflow. The proxy time series follow the observation time series quite well, with the 1993–2011 mean proxy transport of 11.6 ± 3.2 Sv southward, varying from 5.6 Sv during the strong 1997 El Niño to 16.9 Sv during the 2007 La Niña period, which are consistent with previous estimates. The observed Makassar mean transport is 13.0 ± 3.8 Sv southward over 2004–2011, while the SSH proxy (for the same period) gives an ITF mean transport of 13.9 ± 4.1 Sv and the SSH + OBP proxy (for 2004–2010) is 15.8 ± 3.2 Sv.

1. Introduction

The Indonesian seas, with their complex coastline geometry and narrow passages, provide the only pathway for low latitude Pacific water to flow into the Indian Ocean, which is known as the Indonesian throughflow (ITF). The ITF plays an integral role in global ocean thermohaline circulation and directly impacts the basin mass, heat, and freshwater budgets of the Pacific and Indian Ocean with possible influence to the El Niño Southern Oscillation (ENSO) and Asian-Australian monsoon climate phenomena [e.g., Bryden and Imawaki, 2001; Sprintall et al., 2014]. Thus, it is desirable to not only quantify the ITF and its variability, but also monitor it for a longer period of time, and, if possible, to derive a proxy for the ITF transport.

The main ITF pathway from the Pacific into the Indian Ocean is through the Makassar Strait (Figure 1) [Gordon et al., 2010; Susanto et al., 2012; Wajsowicz, 1996]. Some of the ITF passes through an eastern path by way of the Maluku Sea [van Aken et al., 2009]. A smaller inflow, which has larger seasonal variability, is through the Luzon Strait-South China Sea—Java Sea via the Karimata Strait, with influence to the vertical structure of the main ITF [Fang et al., 2010; Qu et al., 2006; Susanto et al., 2010, 2013; Tozuka et al., 2009]. The main exit passages are the Lombok Strait, Ombai Strait, and Timor passages.

It is known that long-term direct measurements of the ITF are expensive and their collection remains logistically challenging. For example, the comprehensive ITF field measurements made through the International Nusantara Stratification and Transport (INSTANT) program involved synchronized coordination and support from five countries (Indonesia, United States, Australia, French, and Netherlands), which only lasted for three years [van Aken et al., 2009; Gordon et al., 2010; Sprintall et al., 2004, 2009]. Therefore, an alternative approach to gauge ITF transport or to develop a proxy is desirable.

Deriving an ITF proxy was first proposed by Wyrski [1987], who suggested estimating ITF variability using the pressure head between the equatorial Pacific and the eastern Indian Ocean. The pressure difference

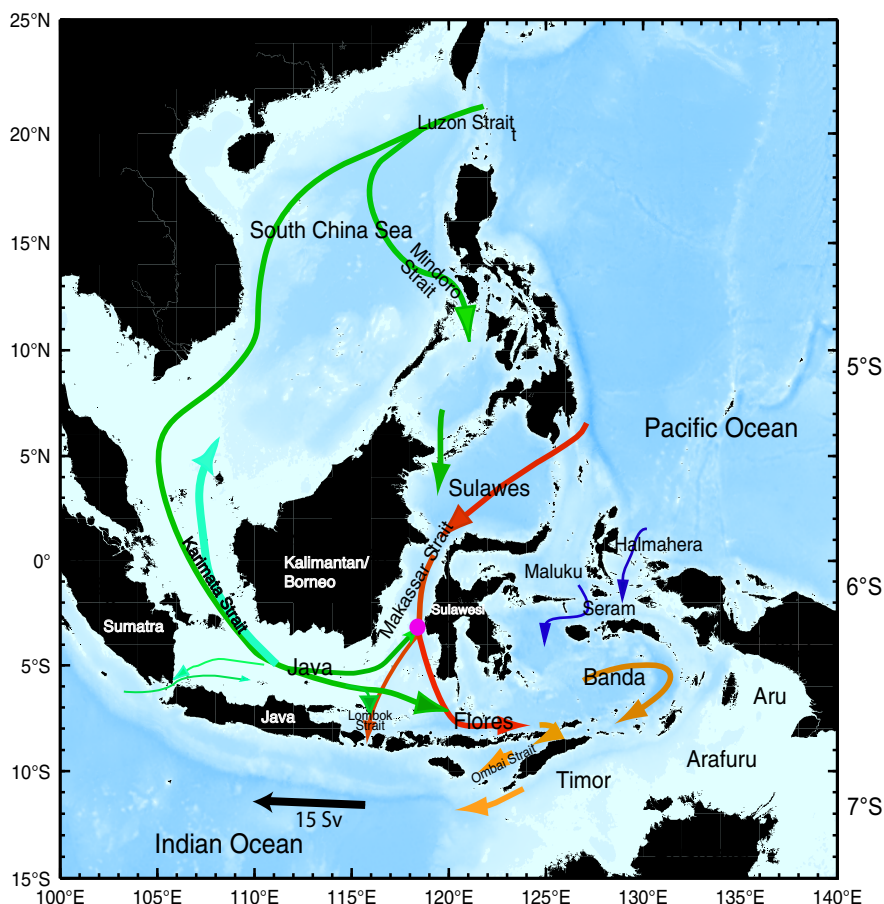


Figure 1. Study area in the Indo-Pacific region and Indonesian Throughflow pathways. Most of the Throughflow (red line) passes through the Makassar Strait. The South China Sea Throughflow is shown in green. The Throughflow via the eastern part of Indonesia/Maluku Sea is shown in blue. All these ITF inputs are mixed in the Banda Sea before exiting into the Indian Ocean, mostly via Timor passage and Ombai Strait (orange).

between the Pacific and Indian Oceans was derived from the observed monthly sea level anomalies at coastal tide stations in Davao/Mindanao Island, the Philippines and Darwin, Australia. Interestingly, *Wyrtki* [1987] found that sea level variations along the south coast of Java would have been more suitable than those at Darwin [*Potemra*, 2005]. However, *Clarke and Liu* [1994] concluded that simple sea level difference between Davao and Darwin could not adequately represent both time series. Later, *Potemra et al.* [1997] used TOPEX/Poseidon (T/P) sea level data and a numerical model to investigate the fluctuations in the ITF volume transport. They presented an index based on the monthly weighted sea level anomalies over four different regions in the western Pacific and the Indian Ocean. Due to insufficient direct observations at that time, accurate estimation of variations in throughflow transport at seasonal and interannual time scales was not yet possible. Using longer T/P sea level time series and a more advanced ocean model, the Simple Ocean Data Assimilation-Parallel Ocean Program (SODA POP 1.2), *Potemra* [2005] revisited their 1997 work based on linear best fit of sea level and its time lag for the five regions of south Java, the western Pacific, Darwin, Davao, and west Sumatra/the equatorial Indian Ocean. He concluded that ITF transport could be estimated using a linear combination of sea level in the Indian Ocean (south Java or Eastern Indian Ocean) minus sea level in Davao, the western Pacific and Darwin. He also noted that ITF transport was forced by several factors in both the Pacific and Indian Oceans at several frequencies. *Susanto et al.* [2007] were able to derive an ITF proxy using sea surface height (SSH) anomalies from T/P altimeters and thermocline depth anomalies along the Lombok Strait. Using the HYbrid Coordinate Ocean Model (HYCOM), *Shinoda et al.* [2012] showed that sea level differences between the eastern Indian Ocean along the coast of Java and Sumatra and the western Pacific (4°N–6°N and 125°E–135°E) had a high correlation with the ITF transport. Recently, *Sprintall and Revelard* [2014] used sea level anomaly in the Pacific and Indian Ocean (six regions)

to derive proxy of ITF based on the observations during INSTANT program (2004–2006) in the exit passages (Lombok Strait, Ombai Strait, and Timor passage). They showed a good agreement between observed and proxy transports. Based on the 18 years proxy time series, there is a significant increase transports through the Lombok Strait and Timor passage. However, a decrease trend is observed in the Ombai Strait. Hence, over the 18 years there is a small decrease 0.5 Sv of the total ITF transport through all exit passages [Sprintall and Revelard, 2014].

In contrast to previous studies, this study has two novelties. First, we use both altimetry SSH and gravimetry ocean bottom pressure (OBP) data, as well as a theoretical formulation of Song [2006] and Qu and Song [2009], to derive the ITF proxy. The reason for using these two data sets is that the ITF transport is not necessarily in the surface layer only; therefore, the OBP data would give complementary information for the total pressure gradient force driving the ITF. We also use the longest-ranging in situ observations of ITF from the Makassar Strait from 2004 to 2011 and earlier measurement in 1996–1998. The continuous Makassar transport from 2004 to 2011 is divided into two parts: validation period (2004–2009) and verification period (2009–2011). The 2004–2009 in situ measurement is used as a baseline in determining optimal correlation regions in the Pacific and Indian Oceans and to validate the proxy derived from the satellite data, whereas the 1996–1998 and 2009–2011 measurements are used as independent time series to test and verify the derived proxy (<http://www.ideo.columbia.edu/res/div/ocp/projects/>). With the availability of 20 year altimetry SSH data and 10 year Gravity Recovery and Climate Experiment (GRACE) ocean bottom pressure (OBP) data, it is time to test the possibility of deriving a long-term ITF proxy for better understanding of the throughflow. Indeed, the theoretical formulation has not been tested with these three data sets. Second, rather than making the assumption that ITF transport is mainly driven by the pressure gradient head (e.g., 2, 4, 5 regions used by Wyrski [1987], Potemra et al., [1997], and Potemra [2005], respectively), we will explore the optimal correlation between the two interior oceans, from 109°E to 180° and from 15°S to 20°N in the Pacific Ocean, and from 70°E to 142°E and from 15°S to 20°N in the Indian Ocean. In the following section, the theoretical base for the discussed approach will be introduced briefly. Section 3 focuses on determining the optimal locations, which will be used for the ITF proxy estimation. Section 4 presents the results, stability of the proxy, and sensitivity analysis. The final section provides a summary and discussions.

2. Theoretical Background

We hypothesize that the magnitude and variability of strait transport varies with both sea-surface height (SSH) and ocean bottom pressure (OBP) gradients between two interconnected oceans. Song [2006] developed a theoretical method by combining the “geostrophic control” formula of Garrett and Toulany [1982] and the “hydraulic control” theory of Whitehead [1989]—allowing the use of SSH and OBP variables for estimating interocean transport, providing a potential use of satellite measurements for obtaining an ITF proxy. However, such a method has not been tested for the ITF transport with in situ measurements. More recently, Qu and Song [2009] revised Song’s [2006] formulation for the Mindoro Strait and the Sibutu Passage between the South China Sea and the Indian Ocean because the “geostrophic control” does not apply to lower latitudes. As noted by Garrett [2004], both geostrophy and friction can limit the flow in a strait. The sea level slope along a strait is then related to a force balance between the pressure gradient, bottom friction, and acceleration. Therefore, we use their Sibutu case because the Makassar Strait is located at the equator. The volume transport, forced by the sea level slope and pressure gradient, also considering the friction effect, can be written as [Qu and Song, 2009]:

$$Q = \frac{r_1 g}{\lambda + r_1 f} H_1 \Delta \eta + \frac{r_2 g}{\lambda + r_2 f} H_2 (\Delta p_b - \Delta \eta) \quad (1)$$

where subscripts 1 and 2 represent the surface and bottom layer, respectively. We use the same bottom friction coefficient as in Qu and Song [2009], $\lambda = C_d U / H_1 \approx 10^{-3} \times 0.5 \times 10^{-2} = 5 \times 10^{-6}$. In the formula, $r = W/L$ is the ratio of the width to the length of the strait, g is gravity, and f is the Coriolis parameter. Furthermore, $\kappa = \text{sign}(\Delta p_b - \Delta \eta)$ determines the gradient direction, and $\Delta \eta$ and Δp_b are the SSH and OBP difference from the Pacific Ocean to the Indian Ocean, respectively. As in Qu and Song [2009] in order to have a combination of bottom pressure and SSH, the bottom pressure variable has been normalized to the thickness of water mass with the same units as the SSH variable. Details on the formulation are referred to in Qu and Song [2009]. The choice of the related parameters will be discussed later.

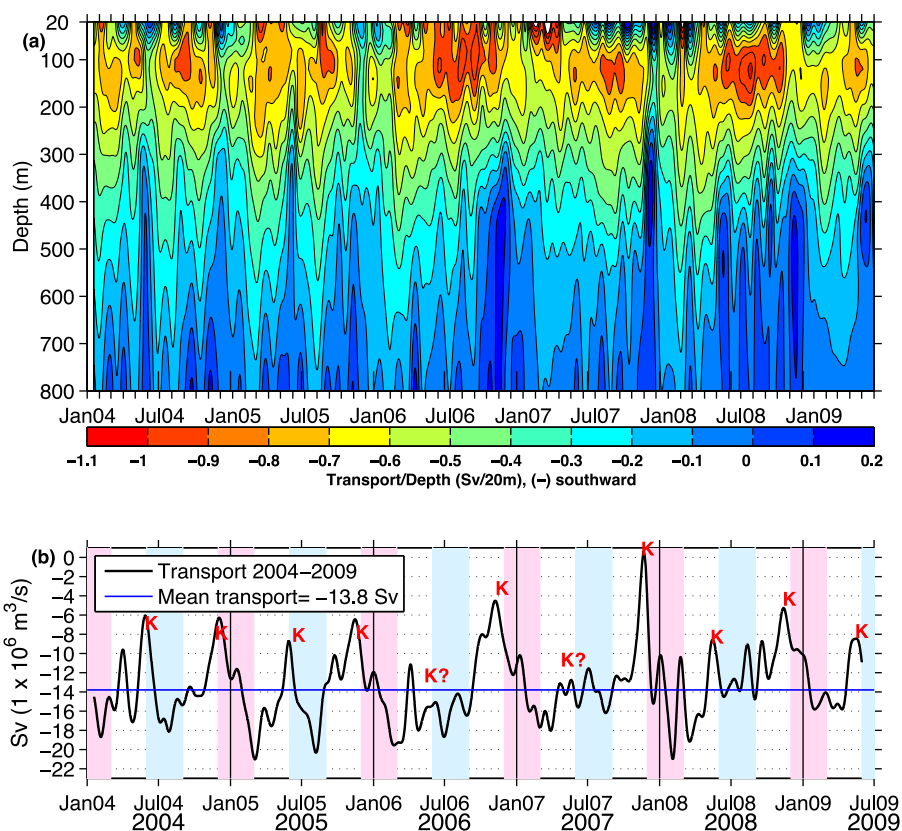


Figure 2. (a) Vertical distribution transport time series per unit depth in the Makassar Strait (Sv/20 m). (b) Total volume transport time series adopted from *Susanto et al.* [2012] (Sv, black). For clarity, a monthly low-pass filter has been applied to the transport time series. The peak of the southeast monsoon is shaded in cyan, while the peak of the northwest monsoon is shaded in magenta. The seasonal grouping is delayed 1 month from monsoonal winds. The intrusions of Kelvin waves (“K”) reduce the mean southward Makassar Strait transport.

In this study, we use the SSH anomaly from a merged weekly product of T/P, Jason-1, ERS-1, and EVISAT, with an averaged horizontal resolution of $1/3^\circ$, produced and distributed by AVISO as part of the Ssalto ground processing segment (<http://www.aviso.oceanobs.com/en/data/tools/citation/index.html>). Although satellite altimetry data have been known as the most precise measurement of the sea level, it still has uncertainties [Ablain et al., 2009]. For people interested in the data errors, we refer to the cited data sources for details. In this study, we have to treat these data as the closest representation of reality because they are the most reliable data we could find. The recent OBP data are obtained from the GRACE mission (<http://podaac.jpl.nasa.gov>). Since its launch in 2002, the GRACE satellite pair has providing monthly estimates of the Earth’s gravity field on spatial scales of a few hundred kilometers. On the seasonal to interannual time scales, changes in the gravity field can be interpreted as changes in a thin layer of water covering the Earth, which over the oceans is equivalent to ocean bottom pressure (OBP) and has been gridded into a regular $1^\circ \times 1^\circ$ globally. The design accuracy of GRACE is equivalent to a surface mass density of 0.1 cm of equivalent water thickness, but the actual accuracy is closer to ~ 1 cm [e.g., Chambers, 2006]. The spatial resolution and accuracy should not affect our study area because we are focusing on the interior ocean signals in large scales. In addition, the monthly OBP data have been interpolated into weekly intervals to be consistent with the SSH and in situ data.

3. Optimal Correlations

The long-term total volume ITF transport has been estimated from various in situ observations from the major inflow and outflow passages [see *Gordon et al.*, 2010, for a full review] and other inflow branches of the ITF, through the South China Sea [*Fang et al.*, 2010; *Susanto et al.*, 2010, 2013] as well as using numerical models [i.e., *Metzger et al.*, 2010; *Shinoda et al.*, 2012]. The Makassar Strait carries most of the ITF and has the

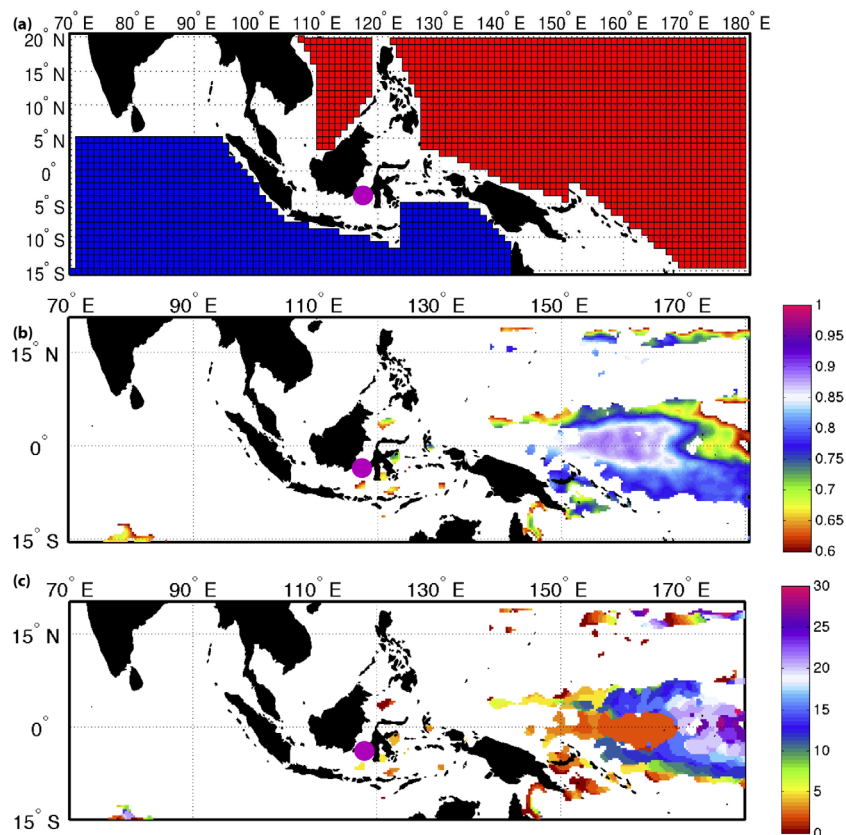


Figure 3. (a) Study regions in the Pacific and Indian Ocean, divided into $1^\circ \times 1^\circ$ horizontal resolution; (b) correlation ($r^2 \geq 0.6$) map; and (c) time-lag map in weeks of the ITF transport at the Makassar Strait and the sea level variations.

longest continuous time series available. The latest estimate of the Makassar Strait transport based on the 2004–2009 field observation was reported by *Susanto et al.* [2012], which can be summarized as follows: (1) the Makassar flow varies from tidal to interannual time scales and is thermocline intensified, with a maximum along-channel velocity of -0.8 m/s near 120 m depth; (2) in addition to ENSO, Indian Ocean Dipole (IOD), and monsoon conditions, ITF in the Makassar Strait is strongly influenced by intrusions of semiannual Kelvin waves from the Indian Ocean; (3) seasonal transport varied from -15.5 Sv ($\text{Sv} = 10^6 \text{ m}^3/\text{s}$) to -9.6 Sv during the northwest monsoon (January–March) to the monsoon transition (October–December); (4) the annual mean transport was southward at 13.3 ± 3.6 Sv [see *Susanto et al.*, 2012, for the detailed calculation]. Figure 2 summarizes the velocity measurements at the Makassar Strait.

The ITF transport is quite complex, and is forced by local and remote forcing in both the Pacific and Indian Oceans [i.e., *Shinoda et al.*, 2012]. Therefore, we do not follow the prior assumption that certain key regions in the Pacific and Indian Oceans are most likely affecting the ITF transport. Instead, we have established an optimal correlation between the Pacific Ocean (from 109°E to 180° and from 15°S to 20°N) and Indian Ocean (70°E to 142°E and from 15°S to 20°N) with the Makassar measurements, by dividing the Pacific and Indian regions into a $1^\circ \times 1^\circ$ horizontal resolution grid. There are 1539 grids in the Pacific (including the South China Sea) and 943 grids in the Indian Ocean, as shown in the red and blue grids, respectively, in Figure 3a.

Before deriving the ITF transport proxy, we need to determine the optimal correlation regions in the Pacific and Indian Oceans with the 2004–2009 Makassar Strait transport. Four approaches have been explored: (1) calculating the maximum cross correlations between sea level at each grid point in both the Pacific and Indian Oceans and in situ measurements from the 2004 to 2009 Makassar Strait; (2) calculating the maximum cross correlations between sea level differences at each grid point in the Pacific and Indian Oceans with the Makassar transport at each vertical level; and (3) calculating the maximum cross correlations between OBP differences as the same as for the sea levels (approach #2). After determining the optimal

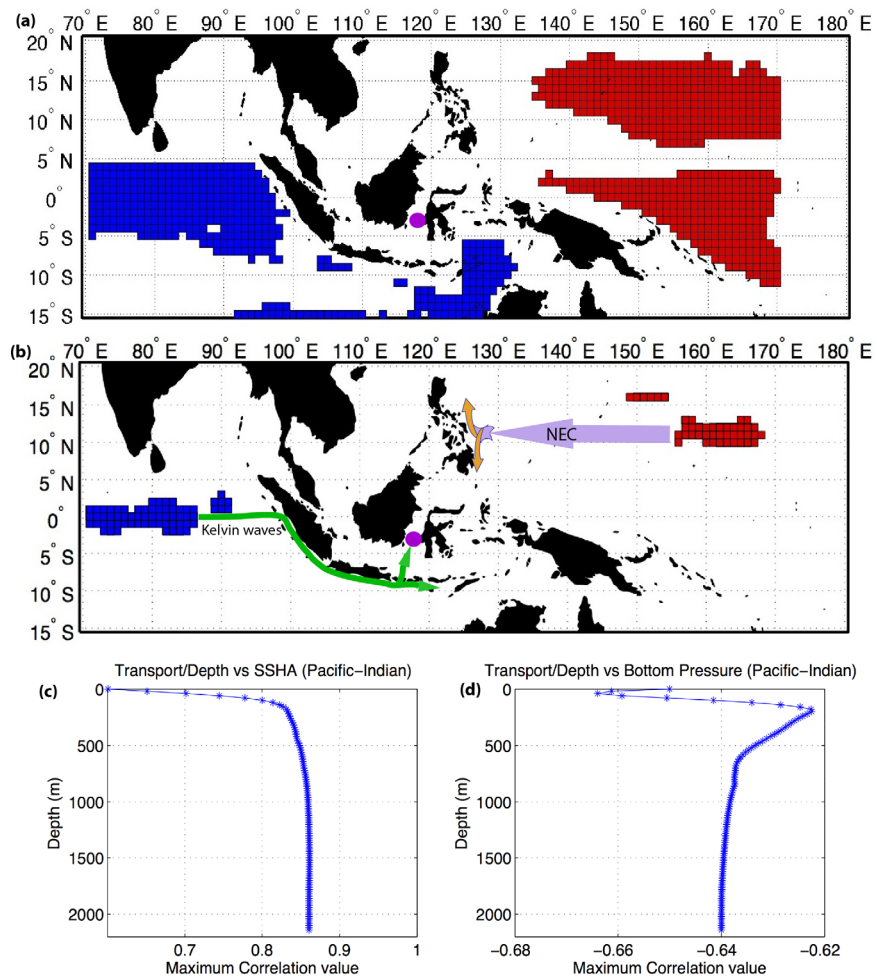


Figure 4. Grids with a positive time lag and a cross-correlation value between the satellite data and in situ transport in the Makassar Strait: (a) for correlation values greater than 0.7 (99% confidence interval, verified using 1000 randomized time series using Monte-Carlo simulations) and (b) for correlation values greater than 0.83 (exceed 99.9% confidence interval), respectively. The mooring location of the in situ observations in the Makassar Strait is shown by the purple circle. (c) Maximum cross-correlation of sea level differences between pair grids (Pacific-Indian Oceans) in Figure 4b, with depth-integrated volume transport in the Makassar Strait every 20 m from the surface to the bottom. (d) Maximum cross-correlation of ocean bottom pressure (OBP) differences between pair grids (Pacific-Indian Oceans) in Figure 4b, with depth-integrated volume transport in the Makassar Strait every 20 m from the surface to the bottom. The sea level differences and ocean bottom pressure differences are calculated between each 1° grid in the Pacific Ocean and each 1° grid in the Indian Ocean. NEC indicates the North Equatorial Current.

correlation regions, we will use the theoretical formula to estimate the ITF transport based on the satellite sea level and ocean bottom pressure data. It should be noted that the Makassar transport is not necessarily the total ITF transport because there are other straits and passages connecting the two oceans. However, the measurements from the Makassar Strait provide the most reliable and longest-range data for us to determine the possible correlations. We will therefore use the determined correlation regions in our theoretical formulation. (4) Finally, verifying the derived proxy with independent Makassar transport in situ observations from 1996 to 1998 and 2009 to 2011.

In the first approach, the weekly sea level time series for each grid in the Pacific and Indian Oceans is correlated with the weekly in situ time series of the total volume transport in the Makassar Strait. The maximum correlation value, for those correlation values greater than 0.6, is shown in Figure 3b. The correlation time lag is shown in Figure 3c, with the positive time lag (in weeks) representing that the Makassar Strait transports lag from the sea level time series. Although the region in the equatorial Pacific from 155°E to 170°E shows the highest correlation with values greater than 0.8 and time lags within 2–5 weeks, sea levels in the Indonesian Seas and the Indian Ocean have weak correlations with the Makassar Strait transport or negative

time lags. These one-side correlations indicate that sea level variability on one side does not necessarily control the throughflow variability because the throughflow variability and strength have to be affected by both oceans. Therefore, the maximum correlation region determined by this approach is not necessarily optimal for deriving the ITF transport.

Because ITF variability depends on both Pacific and Indian Oceans [i.e., Clark and Liu, 1994; Gordon et al., 2010; Meyers, 1996; Potemra et al., 1997; Potemra, 2005; Sprintall et al., 2000; Susanto and Gordon, 2005, 2012; Wijffels and Meyers, 2004; Wyrki, 1987], we only need to determine the optimal correlations between the Makassar Strait transport and the pressure gradients across the two oceans. Our pressure gradient approach is an expansion of Wyrki [1987], Potemra et al. [1997], and Potemra [2005], in the sense that sea level differences between the Pacific and Indian Oceans may control the ITF transport. Rather than making the assumption that ITF transport is mainly driven by the pressure gradient head, we explore the optimal correlation between the two interior oceans, from 109°E to 180° and from 15°S to 20°N in the Pacific Ocean, and from 70°E to 142°E and from 15°S to 20°N in the Indian Ocean. The sea level differences are calculated by differentiating each of the grids in the Pacific Ocean ($N = 1539$ points) with each of the grids in the Indian Ocean ($M = 943$ points), which results in a $N \times M$ array time series. These time series are used to calculate the correlations with the depth-integrated (every 20 m) ITF transport time series in the Makassar Strait. Figures 4a and 4b show a map of grids in which a positive time lag and a correlation value greater than 0.7 and 0.83 are found, respectively. Using Monte-Carlo simulations with a significant correlation threshold value of 0.7 (verified by 1000 randomized time series at 99% confidence interval, Gentle [2003]), we can see that the sea level differences between the north and south equator of the western Pacific and north Australia and along the equatorial Indian Ocean control the ITF transport. However, a significant correlation threshold value of 0.83 (confidence interval exceeds 99.9%) gives an even more confined region in the northern western Pacific and equatorial Indian Ocean (Figure 4b). Then, using the grids in the confined region (Figure 4b), we calculated their cross correlations with the depth-integrated ITF transport every 20 m from the surface to the bottom, which is shown in Figure 4c. The depth-dependant profile shows that the maximum correlation values nearly constant after integrating the ITF transport to the depth of 600 m because there is a Dewakang Sill 550–650 m depth in the south of Makassar Strait that limit the Makassar flow [Gordon et al., 1999].

In the third approach, we calculated the correlations with the OBP data using the same confined grids as in Figure 4b. Figure 4d shows the obtained maximum cross correlations with the OBP differences (Pacific minus Indian Ocean) and with the depth-integrated ITF transport every 20 m from the surface to the bottom. The results indicate that the pressure differences are out of phase with the Makassar ITF transport. The minimum correlation values coincide with the observed velocity maximum [Susanto et al., 2012]. This is as expected because the vertical structure of the Makassar throughflow is not necessarily uniform, as shown in Figure 2.

Based on the correlation results (Figure 4), both sea level and OBP differences between the Pacific Ocean, centered at 162°E and 11°N, and the equatorial Indian Ocean, centered at 80°E and 0°, are found to have a meaningful relationship with the ITF transport variability in the Makassar Strait. Therefore, the central locations have been determined as the optimal locations for the ITF proxy. Besides the statistical correlations, their physical explanations are also considered. For example, the location in the Pacific coincides with the latitude of the westward North Equatorial Current (NEC), where its strength and latitude location varies with ENSO [Qiu and Chen, 2010]. In addition, this region is also associated with off-equatorial Rossby waves, as suggested by White et al. [2003] and McClean et al. [2005], which are also known to influence the ITF inter-annual variation.

In the Indian Ocean, the optimal correlation location is along the equatorial region where the Wyrki Jet is generated [i.e., Clark and Liu, 1994; Iskandar et al., 2005; Qiu et al., 2009; Schiller et al., 2010; Wijffels and Meyers, 2004; Wyrki, 1973]. Such a coincident is consistent with the field measurements that show that the ITF in the Makassar Strait is strongly influenced by intrusions of semiannual Kelvin waves from the Indian Ocean [Sprintall et al., 2000]. The strength of the northward intrusions of Kelvin waves plays an important role in the total ITF transport [Susanto et al., 2012].

4. Transport Estimation

After determining the optimal geographic locations in the Pacific and Indian Ocean that control the Makassar transport, we can use the SSH and OBP data as the ITF proxy base on the determined

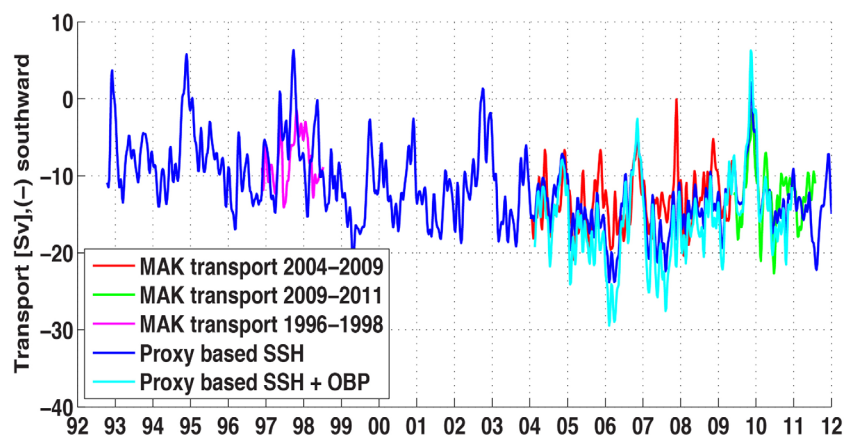


Figure 5. Proxy time series of the ITF transport derived from a combination of satellite SSH and OBP data (blue and cyan). Makassar Strait transport from 2004 to 2009 (red), 1996 to 1998 (magenta), and 2009 to 2011 (green). The blue colors represent proxy time series based on SSH data alone from October 1992 to February 2012, while the cyan colors represent proxy time series based on combined SSH and OBP data from January 2004 to December 2010.

locations and the theoretical approach, which is given in section 2. We choose the following configurations. The Makassar Strait width to length ratios are approximately $r_1 = 0.33$ and $r_2 = 0.03$ [Dinas Hidro oseanografi, 2006]. Based on historical hydrographic data [Boyer *et al.*, 2013], we noticed that density profiles in the Pacific, Makassar Strait, and Indian Ocean change rapidly from the surface to 200 m, with their greatest vertical gradient at about 150 m. Based on the observation, the maximum ITF velocity/transport occurs between 120 and 150 m (Figure 2a) and the bulk Makassar ITF transport is in the top 600 m (Figures 2c and 4c), set by the Dewakang Sill depth 550–650 m in the south of the Makassar Strait [Gordon *et al.*, 1999]. We have also carried out a set of sensitivity analysis by changing various parameters. The best result is obtained when we choose $H_1 = 120$ m as the surface layer thickness, and $H_2 = 450$ m as the bottom layer thickness with 0.22 kg m^{-3} as the density difference between the two layers. Makassar Strait density profiles are derived from CTD data taken during various Indonesian throughflow cruises from 1993 to 2009.

Using a combination of satellite data, in situ measurements, and the simple theoretical formula, we have derived a long-term proxy for the ITF transport from October 1992 to February 2012, as shown in Figure 5. A 5 week Lanczos low-pass filter [Duchon, 1979] was applied to both the weekly satellite and in situ Makassar transport time series. The in situ observations of the Makassar Strait transport from 2004 to 2009 and 1996 to 1998 are in red and magenta, respectively. Meanwhile, the proxy time series of the ITF transport using satellite SSH data are shown in blue, while using a combination of satellite SSH and OBP data are shown in cyan, respectively. It can be seen that the proxy time series follow the observation time series quite well, resolving the intraseasonal, monsoonal, and interannual signals. The significant correlation value between Makassar 2004 and 2009 transport and proxy based on SSH is 0.96 (red line) and confidence interval exceeds 99% (verified using Monte-Carlo simulations on 1000 randomized time series, Gentle [2003]). Similarly, the significant correlation value between 2004 and 2009 Makassar transport and proxy based on SSH + OBP is 0.96, which exceeds the 99% confidence interval. Their threshold significant values are 0.66 and 0.79, respectively.

The 2004–2009 annual mean transport is -13.3 ± 3.6 Sv in the observations [Susanto *et al.*, 2012], slightly lower than the means from the proxies, -13.9 ± 2.5 Sv (SSH only) and -15.9 ± 3.6 Sv (SSH and OBP) for the same period. The ITF proxy using a combination of OBP and SSH is 13% higher than that using only SSH. Because Makassar Strait is the main ITF inflow passage from the Pacific Ocean into the Indian Ocean, the proxy is comparable with the total ITF outflow passages. For example, the 2004–2006 annual mean of the total ITF into the Indian Ocean via the Lombok Strait, Ombai Strait, and Timor passage is 15 Sv [Sprintall *et al.*, 2009], slightly higher than the proxy of SSH only, -14.1 ± 1.8 Sv and slightly lower than that of SSH and OBP, -16.3 ± 3.6 Sv for the same period.

As an independent verification, we have compared the ITF proxy with the latest Makassar measurements from June 2009 to August 2011 [Gordon *et al.*, 2012]. Note that this period of data was not used in the

Table 1. Sensitivity Analysis of the ITF Transport Proxy Using the Theoretical Formula^a

Case	Changing Parameters	ITF Transport Proxy (Sv)			
		SSH 1993–2011		SSH + OBP 2004–2010	
		Mean	Std	Mean	Std
Best	$H_1 = 120 \text{ m}; H_2 = 450 \text{ m}; \Delta\text{Density} = 0.22 \text{ kg m}^{-3}$	11.6	3.2	15.8	3.2
1	$H_1 = 120 \text{ m}; H_2 = 450 + 20\% = 540 \text{ m}$	11.6	3.5	16.3	3.6
2	$H_1 = 120 + 20\% = 144 \text{ m}; H_2 = 450 + 20\% = 540 \text{ m}$	13.9	3.9	18.9	4.0
3	$H_1 = 120 + 20\% = 144 \text{ m}; H_2 = 450 + 40\% = 630 \text{ m}$	13.9	4.1	19.5	4.3
4	$H_1 = 120 + 20\% = 144 \text{ m}; H_2 = 450 + 50\% = 675 \text{ m}$	13.9	4.2	19.8	4.5
5	$H_1 = 120 + 40\% = 168 \text{ m}; H_2 = 450 + 40\% = 630 \text{ m}$	16.2	4.5	22.1	4.6
6	$H_1 = 120 + 40\% = 168 \text{ m}; H_2 = 450 + 50\% = 675 \text{ m}$	16.2	4.7	22.4	4.8
7	Width/Length ratio + 20%	13.0	3.7	17.9	3.8
8	$\Delta\text{Density} + 10\%$	11.0	3.2	15.2	3.3

^a H_1 is the surface layer thickness, and H_2 is the bottom layer thickness.

optimal location or model parameter determination. In this paper, we have calculated the 2009–2011 Makassar total integrated volume transport using similar procedures as in *Susanto et al.* [2012] based on velocity measurements obtained from two ADCPs (upward and downward looking ADCP) and three current meters data (green line in Figure 5). The 2009–2011 mean transport and its standard deviation is -12.3 ± 4.0 Sv. This transport is used as an independent time series to verify, test the stability, and accuracy of the proxy. Indeed, the proxy is accurate and stable. The 2009–2011 proxy (SSH only) mean transport and its standard deviation is -12.4 ± 4.4 Sv. The significant correlation value between the 2009 and 2011 Makassar transport and the proxy based on SSH only is 0.96. Meanwhile the 2009–2010 Makassar transport and the proxy based on SSH + OBP is 0.94. Noting that the processed OBP time series is only available until December 2010. Both significant correlation values exceed 99% confidence intervals with the threshold values of 0.76 and 0.70, respectively, verified by 1000 randomized time series with Monte-Carlo simulations [Gentle, 2003].

The second independent test of the ITF proxy is using the observation period of the ITF *Arlindo* program from 1996 to 1998. The proxy time series also follow the observations fairly well. The significant correlation value between the 1996 and 1998 Makassar transport and the proxy based SSH is 0.78. The significant correlation value exceeds 99% confidence intervals with the threshold values of 0.62, verified by 1000 randomized time series with Monte-Carlo simulations [Gentle, 2003]. The 1996–1998 correlation value is not as high as that for 2009–2011 in situ measurement. However, it is still significant and imply that our proxy is very stable (given the fact that there is gab/no field measurement in the Makassar Strait between 1998 and 2004). The mean total transport in calendar year 1997 is -7.9 Sv in the observations [Susanto and Gordon, 2005] and -5.6 Sv from the proxy. The proxy time series indicate that during the peak of the strong El Niño in 1997/1998, the Makassar Strait transport flowed northward. This is consistent with the strength of El Niño and the strong northward intrusion of Kelvin waves from Indian Ocean [Sprintall et al., 2000; Susanto et al., 2012].

There are some discrepancies between the ITF proxy and the Makassar upper layer measurements in 1996–1998 [Gordon et al., 1999; Susanto and Gordon, 2005]. We speculate that these discrepancies might be due to the following shortcomings: (1) only 3 months of velocity profile in the top 200 m from one of the two ADCPs in the Makassar Strait was recovered [Gordon et al., 1999]. Using statistical analysis and wind data, Susanto and Gordon [2005] filled out the rest of the upper layer velocity profile to estimate the total Makassar Strait transport 1996–1998, which is the data used in this study. Therefore, some uncertainty is possible due to the lack of data; (2) although the Makassar Strait is the main ITF inflow pathway, it does not account for all of the ITF transport; and (3) the satellite estimates are based on a simplified formulation.

Even though the SSH data are available from October 1992 to February 2012, to avoid seasonal bias, the annual mean transport was calculated from January 1993 to December 2011. The seasonal transport over 1993–2011 varies from -14.4 Sv ($\text{Sv} = 10^6 \text{ m}^3/\text{s}$) during the peak northwest monsoon (February) and -13.8 Sv during the peak southeast monsoon (August) to -8.6 Sv during the monsoon transition (October). The 1993–2011 annual mean transport is southward at -11.6 ± 3.2 Sv, which varies from -5.6 Sv during the

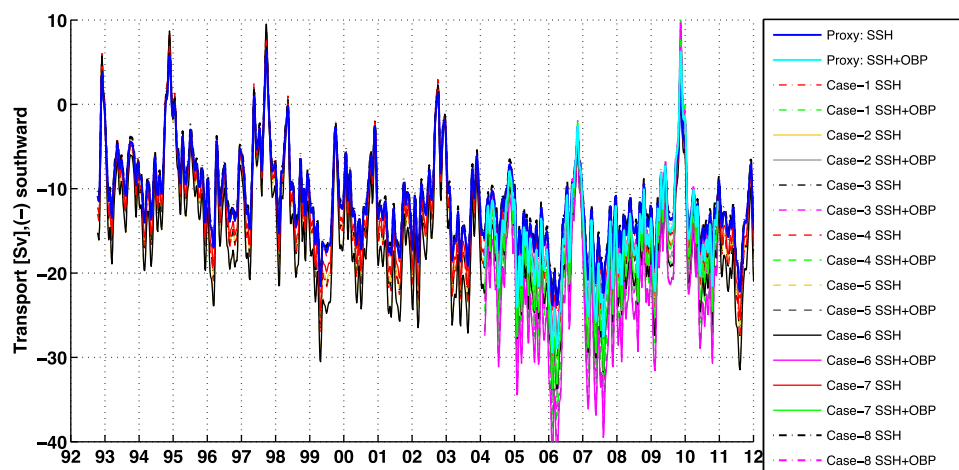


Figure 6. Sensitivity of the proxy time series to the parameters in the theoretical formula. Details and their average transports are given in Table 1.

strong 1997 El Niño with positive IOD event to -16.9 Sv during the 2007 La Niña. The proxy time series show an increased linear trend in ITF transport, with a minimum during the El Niño event in 1992/1993, 1997/1998, 2002/2003, and 2006/2007, respectively. A full explanation can be complicated and is beyond the content of this paper. We refer recent studies of *Sprintall et al.* [2014] and *Sprintall and Revelard* [2014] for the discussions of the ITF response to the changing climate change. Nevertheless, our ITF proxy is a very important result because it provides such a long-term and continuous estimate of the ITF strength and variability, and connects all those ENSO events, which could not be achieved by in situ measurement alone due to logistical and financial challenges.

For completeness, we run sensitivity analysis on our theoretical proxy. It is always difficult to quantify the representation errors of a theoretical formulation because the formation is a simplified or an idealized approximation of reality. Luckily, the theoretical formulation has only a few parameters. Therefore, we have carried out a set of sensitivity analysis to quantify the representation errors of the formulation, as shown in Table 1 and Figure 6. Sensitivity analysis indicates that variability of proxy transport is sensitive to the choice of upper layer thickness and strait geometry, but less sensitive to the changing in lower layer thickness and slightly sensitive to the changing in density different between the Pacific and Indian Ocean. Notice that a set of 10–50% change of parameters results in a change of 20% deviation in the mean transport (e.g., the SSH and OBP column in Table 1), indicating that the formulation is not too much sensitive to the parameters.

5. Summary and Discussions

In summary, we have demonstrated a plausible approach to derive an ITF transport proxy using the 20 year altimetry SSH data and the 10 year GRACE OBP data. The satellite-derived ITF proxy is shown to be consistent with the measurements from the Makassar Strait from 1996 to 1998 and 2004 to 2011, the main pathway of the ITF. Indeed, the ITF proxy is stable and accurate through an independent verification by the 1996–1998 and 2009–2011 Makassar Strait data. Although GRACE has only 10 years of record, its addition shows a sizable effect on the mean and variability of the proxy. This long-term proxy is important and useful because of the role of ITF transport played in the global ocean circulation and climate change. Particularly, our formulation provides a continuous approach to derive the ITF proxy as long as the satellite data are available. Such a continuous record would be difficult to achieve by in situ measurements alone.

The key novelty of this study is the use of the in situ measurements in the Makassar Strait to determine the optimal locations in the Pacific and Indian Oceans for the theoretical formation of *Qu and Song* [2009]. Our results indicate that the SSH and OBP differences between the Pacific Ocean, centered at 162°E and 11°N , and the Indian Ocean, centered at 80°E and 0° , would be the optimal values to derive the ITF proxy volume

and variability. The physical reasons for the high correlation can be explained as follows. The area in the Indian Ocean site is in the tropical region where equatorial Kelvin waves are developed. During the monsoon transition in April and October, semiannual Kelvin waves generated in the tropical Indian Ocean are associated with the Wyrcki Jet, and become coastally trapped Kelvin waves, propagating along the coast of Sumatra-Java and partially entering the Lombok Strait into the Makassar Strait [i.e., Iskandar et al., 2005; Puji-ana et al., 2013; Qiu et al., 2009; Sprintall et al., 2000; Susanto et al., 2000; Wyrcki, 1973].

The area in the Pacific Ocean site is in the region of the westward North Equatorial Current (NEC) and off-equatorial Rossby waves. The strength and latitude of the NEC and westward off-equatorial Rossby waves vary with the El Niño Southern Oscillation (ENSO) [Qiu and Chen, 2010; White et al., 2003; McClean et al., 2005]. Based on observational data, the ITF transport in the Makassar Strait is indeed strongly correlated with ENSO, with strong throughflow during La Niña and weak throughflow during El Niño [i.e., Ffield et al., 2000; Gordon et al., 1999; Meyers, 1996; Susanto and Gordon, 2005; Susanto et al., 2012]. These geographical locations that control the strength and variability of the ITF transport in the Makassar Strait differ from early studies by Wyrcki [1987], Potemra et al. [1997], and Potemra [2005], which deserve a further investigation.

However, we understand the limitations of the simplified formula and the short period of the Makassar measurements used in this study. The satellite approach should be further validated by additional in situ observations. As anticipated, more satellite altimetry data will become available. For example, the joint India and French AltiKa/SARAL mission has been launched recently and is providing new data. The GRACE follow-on with improved technology has been scheduled to launch in 2017. Combining these satellite data will provide more accurate and higher resolution SSH and OBP products, which will allow us to refine our approach. Ideally, it can be used to complement or fill in the gaps of the observations for a continuous ITF proxy for better understanding the ocean climate and validating ocean circulation models.

Acknowledgments

The SSH and OBP data are freely available at NASA web-site (<http://podaac.jpl.nasa.gov>) and the altimeter products are distributed by Aviso (<http://www.aviso.oceanobs.com/duacs/>), while the observation data are available at Lamont Doherty Earth Observatory of Columbia University (<http://www.ldeo.columbia.edu/res/div/ocp/projects>). R.D. Susanto was sponsored by the National Aeronautics and Space Administration (NASA), under contract JPLCIT-1362354. Y. T. Song carried out research at the Jet Propulsion Laboratory, California Institute of Technology, under contract with NASA. We are grateful to our colleagues I. Soesilo, S. Wirasantosa, B. Sulistyono, and R. Adi at the Research and Development Center for Marine and Fisheries (BalitbangKP), Indonesia for their support of the field measurement programs. We appreciate the valuable comments from three anonymous reviewers.

References

- Ablain, M., A. Cazenave, G. Valladeau, and S. Guinehut (2009), A new assessment of the error budget of global mean sea level rate estimated by satellite altimetry over 1993–2008, *Ocean Sci.*, *5*, 1–9.
- Boyer, T. P., et al. (2013), World Ocean Database 2013, in *NOAA Atlas NESDIS 72*, edited by S. Levitus and A. Mishonov, 209 pp., NODC, Silver Spring, Md.
- Bryden, H. L., and S. Imawaki (2001), Ocean transport of heat, in *Ocean Circulation and Climate*, edited by G. Siedler, J. Church, and J. Gould, pp. 455–475, Academic, San Diego, Calif.
- Chambers, D. P. (2006), Evaluation of new GRACE time-variable gravity data over the ocean, *Geophys. Res. Lett.*, *33*, L17603, doi:10.1029/2006GL027296.
- Clarke, A. J., and X. Liu (1994), Interannual sea level in the northern and eastern Indian Ocean, *J. Phys. Oceanogr.*, *24*, 1224–1235, doi:10.1175/1520-0485(1994)024<1224:ISLITN>2.0.CO;2.
- Dinas Hidro-oseanografi (2006), *Peta Selat Makassar-Indonesia*, vol. 126–128, Percetakan Dishidros, Jakarta.
- Duchon, C. (1979), Lanczos filtering in one and two dimensions, *J. Appl. Meteorol.*, *18*, 1016–1022, doi:10.1175/1520-0450(1979)018<1016:LFOAT>2.0.CO;2.
- Fang, G., R. D. Susanto, S. Wirasantosa, F. Qiao, A. Supangat, B. Fan, Z. Wei, B. Sulistyono, and S. Li (2010), Volume, heat and freshwater transports from the South China Sea to Indonesian Seas in the boreal winter of 2007–2008, *J. Geophys. Res.*, *115*, C12020, doi:10.1029/2010JC006225.
- Ffield, A., K. Vranes, A. L. Gordon, R. D. Susanto, and S. L. Garzoli (2000), Temperature variability within Makassar Strait, *Geophys. Res. Lett.*, *27*, 237–240, doi:10.1029/1999GL002377.
- Garrett, C. (2004), Frictional processes in straits, *Deep Sea Res.*, Part II, *51*, 393–410, doi:10.1016/j.dsr2.2003.10.005.
- Garrett, C., and B. Toulany (1982), Sea level variability due to meteorological forcing in the northeast Gulf of St. Lawrence, *J. Geophys. Res.*, *87*, 1968–1978, doi:10.1029/JC087iC03p01968.
- Gentle, J. E. (2003), *Random Number Generation and Monte Carlo Methods*, 2nd ed., Springer, N. Y.
- Gordon, A. L., R. D. Susanto, and A. Ffield (1999), Throughflow within Makassar Strait, *Geophys. Res. Lett.*, *26*, 3325–3328, doi:10.1029/1999GL002340.
- Gordon, A. L., J. Sprintall, H. van Aken, R. D. Susanto, S. Wijffels, R. Molcard, A. Ffield, and W. Pranowo (2010), The Indonesian Throughflow during 2004–2006 as observed by the INSTANT program, *Dyn. Atmos. Oceans*, *50*, 115–128, doi:10.1016/j.dynatmoce.2010.04.003.
- Gordon, A. L., B. A. Huber, E. J. Metzger, R. D. Susanto, H. E. Hurlburt, and T. R. Adi (2012), South China Sea throughflow impact on the Indonesian throughflow, *Geophys. Res. Lett.*, *39*, L11602, doi:10.1029/2012GL052021.
- Iskandar, I., W. Mardiansyah, Y. Masumoto, and T. Yamagata (2005), Intraseasonal Kelvin waves along the southern coast of Sumatra and Java, *J. Geophys. Res.*, *110*, C04013, doi:10.1029/2004JC002508.
- McClean, J. L., D. P. Ivanova, and J. Sprintall (2005), Remote origins of interannual variability in the Indonesian Throughflow region from data and a global Parallel Ocean Program simulation, *J. Geophys. Res.*, *110*, C10013, doi:10.1029/2004JC002477.
- Metzger, E. J., H. E. Hurlburt, X. Xu, J. F. Shriver, A. L. Gordon, J. Sprintall, R. D. Susanto, and H. M. van Aken (2010), Simulated and observed circulation in the Indonesian seas: 1/12_ global HYCOM and the INSTANT observations, *Dyn. Atmos. Oceans*, *50*, 275–300, doi:10.1016/j.dynatmoce.2010.04.002.
- Meyers, G. (1996), Variation of Indonesian through-flow and ENSO, *J. Geophys. Res.*, *101*, 12,255–12,264, doi:10.1029/95JC03729.
- Potemra, J. (2005), Indonesian Throughflow transport variability estimated from satellite altimetry, *Oceanography*, *18*(4), 98–107, doi:10.5670/oceanog.2005.10.

- Potemra, J. T., R. Lukas, and G. T. Michum (1997), Large-scale estimation of transport from the Pacific to the Indian Ocean, *J. Geophys. Res.*, *102*, 27,795–27,812, doi:10.1029/97JC01719.
- Pujiana, K., A. L. Gordon, and J. Sprintall (2013), Intraseasonal Kelvin wave in Makassar Strait, *J. Geophys. Res. Oceans*, *118*, 2023–2034, doi:10.1002/jgrc.20069.
- Qiu, B., and S. Chen (2010), Interannual-to-decadal variability in the bifurcation of the North Equatorial Current off the Philippines, *J. Phys. Oceanogr.*, *40*, 2525–2538, doi:10.1175/2010JPO4462.1.
- Qiu, Y., L. Li, and W. Yu (2009), Behavior of the Wyrтки Jet observed with surface drifting buoys and satellite altimeter, *Geophys. Res. Lett.*, *36*, L18607, doi:10.1029/2009GL039120.
- Qu, T., and Y. T. Song (2009), Mindoro Strait and Sibutu Passage transports estimated from satellite data, *Geophys. Res. Lett.*, *36*, L09601, doi:10.1029/2009GL037314.
- Qu, T., D. Yan, and H. Sasaki (2006), South China Sea throughflow: A heat and freshwater conveyor, *Geophys. Res. Lett.*, *33*, L23617, doi:10.1029/2006GL028350.
- Schiller, A., S. E. Wijffels, J. Sprintall, R. Molcard, and P. R. Oke (2010), Pathways of intraseasonal variability in the Indonesian throughflow region, *Dyn. Atmos. Oceans*, *50*, 174–200, doi:10.1016/j.dynatmoce.2010.02.003.
- Shinoda, T., W. Han, E. J. Metzger, and H. Hurlburt (2012), Seasonal variation of the Indonesian throughflow in Makassar Strait, *J. Phys. Oceanogr.*, *42*, 1099–1123, doi:10.1175/JPO-D-11-0120.1.
- Song, Y. T. (2006), Estimation of interbasin transport using ocean bottom pressure: Theory and model for Asian marginal seas, *J. Geophys. Res.*, *111*, C11S19, doi:10.1029/2005JC003189.
- Sprintall, J., and A. Revelard (2014), The Indonesian throughflow response to Indo-Pacific climate variability, *J. Geophys. Res. Oceans*, *119*, 1161–1175, doi:10.1002/2013JC009533.
- Sprintall, J., A. L. Gordon, R. Murtugudde, and R. D. Susanto (2000), A semiannual Indian Ocean forced Kelvin wave observed in the Indonesian seas in May 1997, *J. Geophys. Res.*, *105*, 17,217–17,230, doi:10.1029/2000JC900065.
- Sprintall, J., S. Wijffels, A. L. Gordon, A. Ffield, R. Molcard, R. D. Susanto, I. Soesilo, J. Sopaheluwakan, Y. Surachman, and H. M. van Aken (2004), A New International Array to Measure the Indonesian Throughflow: INSTANT, *EOS Trans. AGU*, *85*(39), 369–376, doi:10.1029/2004EO390002.
- Sprintall, J., S. E. Wijffels, R. Molcard, and I. Jaya (2009), Direct estimates of the Indonesian throughflow entering the Indian Ocean: 2004–2006, *J. Geophys. Res.*, *114*, C07001, doi:10.1029/2008JC005257.
- Sprintall, J., A. L. Gordon, T. Lee, J. T. Potemra, K. Pujiana, and S. E. Wijffels (2014), The Indonesian seas and their role in the couple ocean-climate system, *Nat. Geosci.*, *7*, 487–492, doi:10.1038/ngeo2188.
- Susanto, R. D., and A. L. Gordon (2005), Velocity and transport of the Makassar Strait throughflow, *J. Geophys. Res.*, *110*, C01005, doi:10.1029/2004JC002425.
- Susanto, R. D., A. L. Gordon, J. Sprintall, and B. Herunadi (2000), Intraseasonal variability and tides in Makassar Strait, *Geophys. Res. Lett.*, *27*, 1499–1502, doi:10.1029/2000GL011414.
- Susanto, R. D., A. L. Gordon, and J. Sprintall (2007), Observations and proxies of the surface layer Throughflow in Lombok Strait, *J. Geophys. Res.*, *112*, C03592, doi:10.1029/2006JC003790.
- Susanto, R. D., G. Fang, I. Soesilo, Q. Zheng, F. Qiao, Z. Wei, and B. Sulisty (2010), New surveys of a branch of the Indonesian throughflow, *Eos Trans. AGU*, *91*(30), 261–263, doi:10.1029/2010EO300002.
- Susanto, R. D., A. Ffield, A. L. Gordon, and T. R. Adi (2012), Variability of Indonesian throughflow within Makassar Strait throughflow: 2004 to 2009, *Geophys. Res. Lett.*, *117*, C09013, doi:10.1029/2012JC008096.
- Susanto, R. D., Z. Wei, T. R. Adi, B. Fan, S. Li, and G. Fang (2013), Karimata throughflow from December 2007 to November 2008, *Acta Oceanol. Sin.*, *32*(5), 1–6, doi:10.1007/s13131-013-0307-3.
- Tozuka T., T. Qu, Y. Masumoto, and T. Yamagata (2009), Impacts of the South China Sea throughflow on seasonal and interannual variations of the Indonesian Throughflow, *Dyn. Atmos. Oceans*, *47*, 73–85, doi:10.1016/j.dynatmoce.2008.09.001.
- van Aken, H. M., I. S. Brodjonegoro, and I. Jaya (2009), The deep water motion through the Lifamatola passage and its contribution to the Indonesian throughflow, *Deep Sea Res., Part I*, *56*, 1203–1216, doi:10.1016/j.dsr.2009.02.001.
- Wajswowicz, R. C. (1996), Flow of a western boundary current through multiple straits: An electrical circuit analogy for the Indonesian Throughflow and archipelago, *J. Geophys. Res.*, *101*, 12,295–12,300, doi:10.1029/95JC02615.
- White, W. B., Y. M. Tourre, M. Barlow, and M. Dettinger (2003), A delayed action oscillator shared by biennial, interannual, and decadal signals in the Pacific basin, *J. Geophys. Res.*, *108*(C3), 3070, doi:10.1029/2002JC001490.
- Whitehead, J. A. (1989), Internal hydraulic control in rotating fluids: Applications to oceans, *Geophys. Astrophys. Fluid Dyn.*, *48*, 169–192, doi:10.1080/03091928908219532.
- Wijffels, S. E., and G. Meyers (2004), An intersection of oceanic waveguides: Variability in the Indonesian Throughflow region, *J. Phys. Oceanogr.*, *34*, 1232–1253, doi:10.1175/1520-0485(2004)034<1232:AIOOWV>2.0.CO;2.
- Wyrтки, K. (1973), An equatorial jet in the Indian Ocean, *Science*, *181*, 262–264, doi:10.1126/science.181.4096.262.
- Wyrтки, K. (1987), Indonesian throughflow and the associated pressure gradient, *J. Geophys. Res.*, *92*, 12,941–12,946, doi:10.1029/JC092iC12p12941.